V. Karakoç et al. / Hacettepe J. Biol. & Chem., 2024, 52 (4), 217-236

Research Article

Hacettepe Journal of Biology and Chemistry

journal homepage: www.hjbc.hacettepe.edu.tr

Removal of As(V) from Water with Cryogels Prepared By Molecular Imprinting Technique

Moleküler Baskılama Tekniği İle Hazırlanmış Kriyojeller ile Sulardan As(V) Giderimi

Veyis Karakoç[1*], Hatice Bektaş[2], Deniz Türkmen[3] and Adil Denizli[3]

[1]Vocational School of Health Services, Çankırı Karatekin University, Çankırı, Turkey.

[2]Department of Environmental Engineering, Hacettepe University, Ankara, Turkey.

[3]Department of Chemistry, Hacettepe University, Ankara, Turkey.

ABSTRACT

The aim of this study is the selective removal of As(V) ions, the most abundant form of arsenic in drinking water and especially in surface water. For this purpose, a super macroporous polymeric cryogel column was prepared by molecular imprinting technique. Due to the high affinity of arsenic to sulfhydryl (-SH) functional groups, MAC was chosen as the functional monomer. The MAC monomer was synthesized from the amino acid cysteine as a functional monomer. The physicochemical properties of the HEMA-based synthesized poly(HEMA-MAC) cryogel were determined by Fourier transform infrared spectrophotometer (FTIR), scanning electron microscopy (SEM), surface area measurement, elemental analysis and swelling test. Adsorption studies of water were carried out in a continuous flow system. In order to determine the optimum conditions for removal of As(V) ions from water, different parameters such as pH, flow rate, temperature, initial ion concentration and contact time were studied. The maximum As(V) removal of poly(HEMA-MAC) cryogel was 189.4µg/g polymer at pH 5.0 and 15ppm concentration. Selectivity studies were performed in the presence of PO_4^{3-}, SO_4^{2-}, and NO3- ions. According to the relative k values obtained from the selectivity experiments, the As IIP cryogel exhibits 1.52 times higher selectivity for As(V) ion than PO_4^{3-} ion, 2.61 times higher selectivity for SO_4^{2-} ion and 1.53 times higher selectivity for NO_3^- ion than NIP cryogel. From theoretical calculations, it was found that As(V) adsorption fit Langmuir isotherm and the adsorption process obeyed pseudo-second order kinetics.

Key Words

Arsenic removal, kriyojel, Ion Imprinting, adsorption, cystein.

ÖZ

Bu çalışmanın amacı içme sularında ve özellikle yüzey sularında en yaygınarsenik türü olan As(V) iyonlarını seçimli olarak uzaklaştırılmasıdır. Bu amaçla moleküler baskılama tekniği kullanılarak süpermakro-gözenekli polimerik kriyojel kolonu hazırlandı. Arseniğin sülfidril (–SH) fonksiyonel gruplarına olan yüksek afinitesi nedeni ile fonksiyonel monomer olarak MAC seçildi. MAC monomeri sistein aminoasidinden sentezlendi. HEMAbazlı sentezlenen Poli(HEMA-MAC) kriyojeli fizikokimyasal özellikleri SEM yüzey alanı, şişme ve FTIR ile karakterize edildi. Sulardan adsorpsiyon çalışmaları sürekli sistemde gerçekleştirildi. Sentezlenen poli(HEMA-MAC)kriyojelinin sulardan As(V) iyonunu giderimi için optimum koşullar belirlemek adına pH, akış hızı, sıcaklık, başlangıç iyon konsantrasyonu, etkileşim zamanı gibi farklı parametreler çalışıldı. Poli(HEMA-MAC) kriyojelinin maksimum As(V) giderimi pH: 5.0'da ve 15ppm derişimde 189.4µg/g polimer olarak gerçekleşti. Seçicilik çalışmaları-PO_4^{3-}, SO_4^{2-} ve NO_3^- iyonlarının varlığında yapıldı. Seçicilik deneylerinden elde edilen bağıl k değerlerine göre As IIP kriyojeli NIP cryogel'e göre, As(V) iyonunaPO_4^{3-}-iyonundan 1,52 kat, SO_4^{2-} iyonu için 2,61 kat ve NO_3^- iyonu için 1,53 kat daha fazla seçicilik göstermektedir. Teorik hesaplamalardan As(V) adsorpsiyonunun Langmuir izotermine uygun olduğu ve adsorpsiyon sürecinin yalancı ikinci derece kinetiğe uyduğu bulunmuştur.

Anahtar Kelimeler

Arsenik giderimi, kriyojel, İyon Baskılama, adsorpsiyon, sistein.

Article History: Mar 9, 2024; Revised: Apr 29, 2024; Accepted: May 15, 2024; Available Online: Oct 2, 2024.

DOI: https://doi.org/10.15671/hjbc.1446425

Correspondence to: V. Karakoç, Vocational School of Health Services, Çankırı Karatekin University, Çankırı, Turkey.

E-Mail: veyiskarakoc@karatekin.edu.tr

INTRODUCTION

The concentration of arsenic in surface waters and groundwater is increasing due to human and anthropogenic reasons day by day. According to the World Health Organization (WHO) and International Agency for Research on Cancer (IARC), Arsenic is one of the most toxic heavy metals found in water [1,2]. In 1993, WHO reduced the maximum acceptable value of arsenic in water from 50ppb to 10ppb due to the negative effects of arsenic on human health [3,4].

Arsenic pollution is the most common heavy metal pollution on earth. Water with high levels of arsenic contamination has been reported in many countries [1-4]. Particularly India and Bangladesh are among the top countries that has regions with high populations exposed to arsenic-contaminated waters. Long-term exposure to arsenic causes many diseases such as cardiovascular diseases, diabetes, nervous system diseases, anorexia and vomiting, hyperpigmentation, hypopigmentation, keratosis, arsenicosis, black foot disease and cancer [1,5].

Arsenic can be found in water in different oxidation states such as (3-), (0), (3+) and (5+) depending on the redox potential of the water and its pH. The most toxic form of arsenic is the 3+ form. While trivalent form of arsenic (arsenite, As(III)) is commonly found in the groundwater, pentavalent form of arsenic (arsenate, As(V)) is mostly found in drinking water and surface waters [6,7]. In removing arsenic from drinking water, studies have been carried out to remove the As (V), which is charged in a wide pH range. In large-scale arsenic removal systems in cities, arsenic species in water are converted to the 5+ form, which can be more easily removed, by adding oxidizing agents such as ozone [8,9].

Various methods such as coagulation, filtration, oxidation, ion exchange and adsorption are used to remove arsenic from water [10-16]. When determining which arsenic removal method(s) to use, issues such as the amount of water to be treated, flow rate, and cost of the method are taken into consideration. Each of these methods, which are very different from each other, has advantages as well as disadvantages. According to the World Health Organization, the adsorption method is the most applicable method because it is cheap, usable and harmless [17].

Adsorption is the most common method used in arsenic removal. The adsorption method is mostly used in small-scale treatment processes. Compared to other methods, the adsorption method stands out with its features such as being simple, low-cost, effective, easy-to-use, efficient and recyclable [17-20].

Cryogels are new generation polymeric adsorbents with macropores. They have high surface areas due to their spongy structure. Due to these features, they allow even viscous liquids to pass easily. They can swell in water and can easily hold water approximately 10 times their dry weight [21,22]. Cryogels can be synthesized in different forms such as membrane or column forms by adding an initiator to the water monomer mixture and keeping it at -20 C for 24 hours. The polymerization process continues while the water phase forming the micro-phase crystallizes at low temperature and creates pores in the structure. At the end of the process, the porous structure is obtained by melting and removing the water phase in the ice-polymer mixture left at room temperature. In addition to being frequently preferred in separation and purification processes, cryogels have also attracted the attention of researchers in tissue engineering, drug delivery systems and biotechnology [23-30].

Molecular imprinting technique is a technique used to synthesize polymeric matrices used in processes requiring high recognition ability [31,32]. In this technique, surfaces that recognize the target molecule are created by the polymerization process in the presence of the target analyte and monomer mixture in the same medium. Therefore, the target analyte is trapped inside the polymeric structure. After polymerization, the target analyte is removed from the polymeric structure by using appropriate desorbing agents. By removing the analyte from the polymeric structure, analyte-specific 3D cavities are obtained in the structure. Adsorption occurs by these cavities formed on the surface of the polymer, which recognize the target analyte using weak secondary interactions such as electrostatic, hydrophobic or hydrogen bonds [33]. Polymers prepared using the molecular imprinting technique are used in cell and sensor applications, drug development and release systems, as well as separation and purification [34-36].

In this study, cryogels with –SH groups on their surfaces were prepared using the ion imprinting technique to remove As(V) ions, the most common species of arsenic in

drinking water. Arsenic has a high affinity for sulfur and forms complexes with –SH molecules of enzymes and proteins in biological systems [37-41]. For these reasons, MAC monomer was first synthesized from the cysteine amino acid. Then, in order to use the ion imprinting technique, the MAC-As complex was formed and polymerization was performed. The use of –SH-containing monomer in polymerization eliminates the subsequent ligand immobilization step and prevents ligand leakage. Studies were carried out to determine the As(V) removal performance from aqueus solutions of synthesized As-IIP polymeric cryogels.

MATERIALS and METHODS

Materials

The main ingredients for the preparation of MAC monomer and As IIP cryogel were methacryloyl chloride and L-cysteine hydrochloride, 2-hydroxyethyl methacrylate (HEMA), ethylene glycol dimethacrylate (EGDMA), ammonium persulfate (APS) and N,N,N,N-tetramethyldiamine (TEMED) was obtained from Sigma (Sigma Chemical Co., USA) and stored at 4°C until use. $Na_2HAsO_4.7H_2O$ arsenic salts were respectively used as the source of As(V) ions determined as target ions, and they were purchased from Merck (MERCK Co., Darmstadt, Germany). Other chemicals used in the study were of analytical purity and were obtained from Merck (Darmstadt, Germany). Water used in experiments was purified using a reverse osmosis Barnstead (Dubuque, IA) ROpure LP® unit with a high-flux cellulose acetate membrane (Barnstead D2731) followed by a Barnstead D3804 NANOpure® organic/colloid removal unit and an ion exchange packed column system. The conductivity of the resulting deionized water is 18.2 MΩ/cm. The glass materials used in the experiments were cleaned by soaking them in 4M nitric acid overnight.

Experimental Methods

Synthesis of N-Methacryloyl-(L)-Cysteine (MAC) Monomer

MAC was chosen as the functional monomer for the preparation of As-IIP cryogel. The following method was applied [42] for the synthesis of MAC; 5.0 g L-cysteine and 0.2 g hydroquinone were mixed in 100 mL dichloromethane solution. This solution was cooled to 0°C and 12.7 g of triethylamine was added to the solution. 5.0 mL of methacryloyl chloride was slowly added to this solution and then magnetically stirred at room temperature for 2 hours. At the end of the chemical reaction period, hydroquinone and unreacted methacryloyl chloride were extracted with 10% NaOH solution. The liquid phase was evaporated in a rotary evaporator. MAC was crystallized in ether-cyclohexane mixture and then dissolved in ethyl alcohol.

Preparation of MAC-As Complex

In the first step of the preparation of the MAC-As precomplex, the functional MAC monomer synthesized was complexed with As(V) ions at a ratio of 1/3 mole (As/MAC). Sodium arsenate ($Na_2HAsO4.7H2O$) salts were used to form MAC-As complex. To prepare MAC-As complexes, 1.0 mmol sodium arsenate ($Na_2HAsO_4.7H_2O$) (0.312g) was dissolved in 15 mL of ethanol/water solution. Then, 2.0 mmol of solid MAC (0.380 g) was added slowly to these mixtures and stirred continuously for 3 hours at room temperature. Then, the formed metal-monomer complexes were precipitated, filtered, washed with 99% ethanol (250 ml) solution and dried in a vacuum oven at 30°C for 24 hours. In this way, MAC-As complexes were prepared.

Preparation of As-IIP Supermacroporous Cryogel

Supermacroporous cryogel is prepared by the free radical polymerization method as follows[43]; First, 1.3 mL of HEMA monomer and 20 mg of MAC-As complex are dissolved in 5 mL of deionized water. Then, the second solution is created by dissolving 0.283 g of MBAAm in 10 mL of deionized water. After the dissolution processes, these two solutions are mixed. Supermacroporous cryogels are mixed for 1 minute by adding 25 µL TEMED and 20 mg APS (1%, w/v), and the solutions are immediately poured into 5 mL plastic syringes with closed bottoms and left to polymerize by freezing at -18°C for 24 hours. The frozen polymer ice mixture is brought to room temperature and the ice is melted, thus supermacroporous As-IIP cryogel is obtained. The prepared cryogel is washed with 200 mL water/ethanol, then arsenic ions are removed from the cryogel with 50 mM EDTA (pH 4.0) solution. Thus, cavities specific to As(V) ions are obtained. Non-As imprinted (NIP) cryogel was prepared under the same conditions without adding As(V)ions to the polymerization medium. The synthesized supermacroporous cryogels are stored in 0.02% sodium azide (NaN_3) solution at +4°C until use.

Characterization Studies

Investigation of Swelling Properties of Cryogels

The swelling properties of cryogels were examined using at least 3 identical cryogels samples. To determine the cryogel equilibrium swelling ratio, the dry cryogel sample was weighed with an accuracy of ±0.0001 and placed in a container containing 50 ml of pure water. The container was kept in a water bath at constant temperature (25 ± 0.5°C) for 24 hours. The same cryogel sample was taken from water, and the excess water on its surface was gently removed with the help of filter paper and weighed. The weight of dry and wet cryogel was recorded separately and the water content was calculated with the help of Equation 1.

$$\textit{Equilibrium swelling ratio}\ (\%) = [(M_S - M_D)/M_S] \times 100 \qquad (1)$$

M_S and $M_D$refer to the swollen and dry weights (g) of the cryogel, respectively.

Structure Analysis with FTIR

FTIR structure analyzes of MAC monomer and As-MAC complexes, As -IIP cryogels were examined using FTIR 8000 Series, Shimadzu brand spectroscopy device (FTIR 8000 Series, Shimadzu, Shimadzu Corp., Japan). Before analysis, monomer and polymer samples were dried in a vacuum oven for 24 hours. FTIR spectra of the prepared samples were taken in the wave number range of 4000-400 cm^{-1}.

Surface Morphology Analysıs

The surface and internal section structural analysis of the synthesized cryogels were examined by scanning electron microscopy (SEM). For this purpose, cryogel polymer sections were attached to the aluminum plate with a conductive adhesive. Then, the sample surfaces were made conductive by coating them with 20Å thick metallic gold under vacuum. The prepared samples were placed in the SEM sample holder and photographs were taken at various magnifications (Carl Zeiss Microscoy GmbH 73447 Oberkochen Germany).

Surface Area Measurements

The pore volume and average pore diameter of As-IIP and NIP cryogels were determined by mercury porosimetry (Carlo Erba Model 200, Italy). For this, firstly, the cryogels, which were kept in ionized water, were swollen and then frozen at -20°C and dehydrated in the lyophilizer. Specific surface areas of dry samples were determined by the multi-point BET method.

Elemental Analysis

Elemental analysis was performed to determine the amount of MAC in the synthesized As-IIP cryogels. 1 mg of cryogel was placed in the aluminum cell of the elemental analyzer (Leco, CHNS-932, USA) and weighed with an accuracy of ±0.0001 g. The weighed cryogel sample was placed in the device, and as a result of the burning process, the carbon (C), hydrogen (H), oxygen (O), nitrogen (N) and sulfur (S) rates of the sample were determined as percentage (%).

Adsorption Experiments

As(V) ion solution was continuously pumped into the As-IIP, cryogel column using a peristaltic pump. Before the experimental studies, the cryogel column was made ready for the experiment by passing 50 ml of ionized water and conditioning it for 30 minutes. During the adsorption experiments, 50mL As(V) solution was used in the continuous system. The effects of initial As(V) concentration, flow rate, pH of the medium, temperature and adsorption time on the adsorption capacity were examined. The effect of pH on adsorption capacity was examined between pH 4.0 and 9.0. The effect of initial As(V) concentration on adsorption capacity was examined by varying the As(V) concentration between 0.05-15 mg/L. The effect of flow rate on adsorption capacity was examined at different flow rates ranging from 0.5-3.0 mL/min. The effect of temperature on adsorption capacity was examined between 4.0 and 40°C.

The adsorption amount of As(V) adsorbed to the cryogel was calculated by determining the As(V) concentrations in the solution before and after As-IIP interacted with the cryogel (Equation 2).

$$Q=[(C_O - C)V]/m \qquad (2)$$

Here, Q is the amount of As(V) ion adsorbed on the cryogel unit weight (µg/g); C_o ve Crepresent the initial and final As(V) concentrations (µg), respectively; V refers to the solution volume (mL) and m refers to the weight of As-IIP and NIP cryogel (g).

As(V) concentrations in aqueous solutions were determined by flame atomic absorption spectrophotometer (Analyst 800, Perkin Elmer, USA). Deuterium background correction has been made and the spectral slit width is 0.7 nm. Operating current/wavelength is 10 mA/193.7 nm. The sensitivity of the device was periodically checked with standard As(V) solution. The

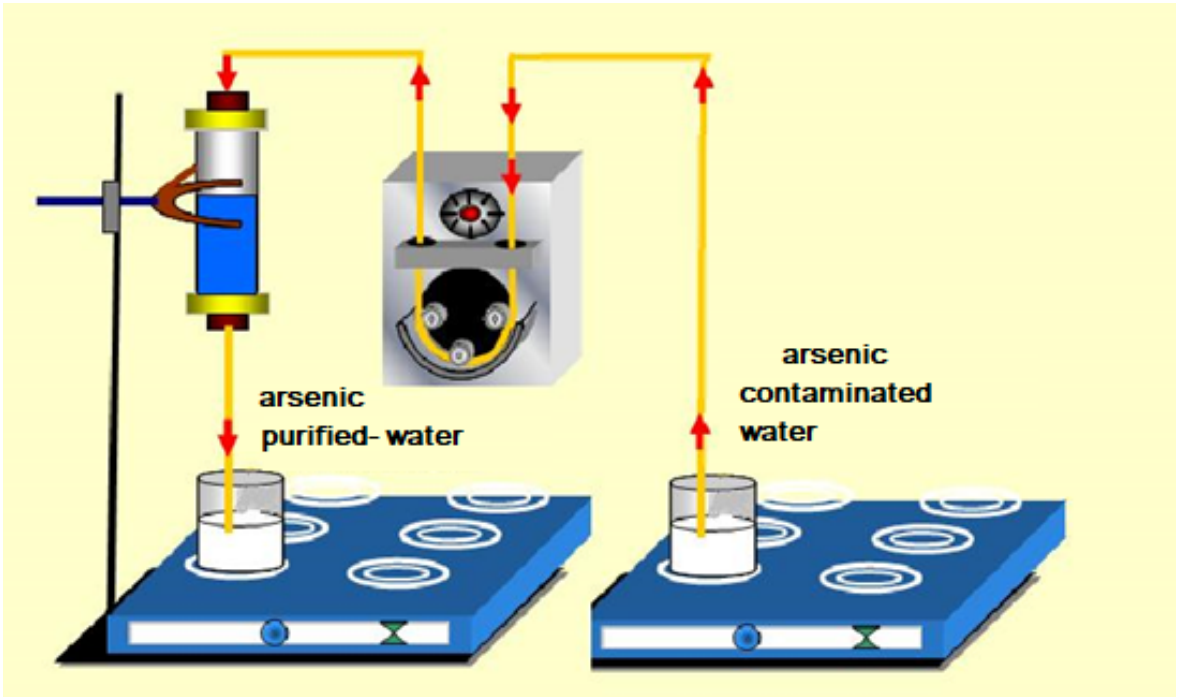

Figure 1. Continuous flow system experimental setup in which adsorption processes are carried out.

experiments were repeated at least three times. The confidence interval was kept at 95%. Standard statistical methods were applied to calculate mean values and standard deviation for each data set. The concentration corresponding to the signal that can be differentiated from the blank value is the lowest concentration that the method can detect. An analytical method appears to be more adequate the lower the concentration it can detect.

Selectivity Studies

Competitive adsorption experiments were carried out to demonstrate the selectivity of the As-IIP cryogel. PO_4^{3-}, SO_4^{2-} and NO_3^- ions were used as competitive anions. $HAsO_4$-oxy-anion was added to the competitive anion mixtures. In selectivity experiments using As-IIP and NIP cryogels, solutions containing anion mixtures at 5 ppm (mg/L) concentration (total volume: 100 mL) were studied at a flow rate of 1 mL/min for 2 hours. At the end of the adsorption period, the concentration of anions in the solution was determined by Ion-LC (Dionex Corporation, USA) and $HAsO_4$-oxy-anions were determined by ICP-MS.

The distribution and selectivity coefficients of the $HAsO_4^-$ oxy-anion relative to the PO_4^{3-}, SO_4^{2-} and NO_3^- anions, respectively, were determined according to the following equation:

$$K_d = [(C_i - C_f) / C_f]. V/m \quad (3)$$

In the equation above, K_d is the distribution coefficient; C_i and C_f refer to the initial and final concentrations of anions and oxy-anions (mg/L), V refers to the volume of solution used (mL), and m refers to the dry weight of the cryogel used (g).

The selectivity coefficient for the binding of an oxy-anion in the presence of competitive anions is obtained from the equilibrium binding data according to Equation 4.

$$k = k_{target}/k_{competitor} \quad (4)$$

The ratio of adsorption studies performed with As-IIP to NIP adsorption studies, which is expressed as control, allows comments about the relative selectivity coefficient of As-IIP. The relative selectivity coefficient is expressed in Equation 5.

$$k' = k_{impirinted}/k_{control} \quad (5)$$

Desorption and Reusability

50 mM EDTA (pH 4.0) solution was used as a desorption agent for the desorption of As(V) ions adsorbed on the As-IIP cryogel. Before starting the desorption process, the As-IIP cryogel was first washed with deionized water to remove impurities and other unbound residues and then equilibrated with DI. water for 1 hour. Under these conditions, the As-IIP cryogel was desorbed with 100 mL of desorption solution for 2 h at room temperature. After the desorption process, the cryogel to be used again, it was washed with deionized water and the As-IIP cryogel was brought into equilibrium again by providing adsorption conditions (such as pH, temperature). In order to determine the reusability of As-IIP cryogel, the adsorption-desorption process was repeated at least 10 times using the same cryogel. The desorption rate of As-IIP cryogel was calculated using Equation 6 from the amount of As(V) adsorbed and desorbed onto the cryogels;

$$\% \text{ Desorption} = \frac{\text{As(V) released into the desorption medium}}{\text{Adsorbed As}} \times 100 \quad (6)$$

RESULTS and DISCUSSION

Supermacroporous As(V) Imprinted (As-IIP) Cryogels

(MAC) monomer was chosen as the functional monomer for the selective removal of As(V)ions from water. In removing As(V) ions from water, the chelation of these ions with the –SH (sulhydryl) group in the MAC monomer was used. The advantage of using MAC as monomer; unlike other adsorption systems, it eliminates the activation steps for ligand immobilization and ligand leakage problems [44]. Figure 2 shows the schematization of the coordination bond formed by As(V) ions with sulfur and oxygen atoms in the functional monomer structure.

Characterization Studies

Structure Analysis with FTIR

For FTIR spectrum analysis of MAC-As complexes, complexes formed using 1 mmol As(V) salt and 3 mmol MAC monomer were used. Spectra of the prepared sample were taken on the FTIR device in the wave number range of 4600-400 cm^{-1}.

In the FTIR spectrum of MAC monomer, the characteristic carboxylic acid C=O stretching band is at 1747 cm^{-1}, amide I and amide II absorption bands are at 1674 $cm^{-1}$and 1520 cm^{-1}, the weak S-H stretching band is at 1089 $cm^{-1}$and 969 cm^{-1}. In the FTIR spectra of As-MAC complexes, it is seen that the peak intensities of the MAC monomer decrease in the S-H stretching bands at 1128 $cm^{-1}$and 967cm^{-1} due to the formation of coordinated covalent bonds. In addition, it was observed that some peaks shifted to the higher frequency region with the decrease in electron density due to the complex formed in the intensities of other peaks in the MAC monomer (Figure 3).

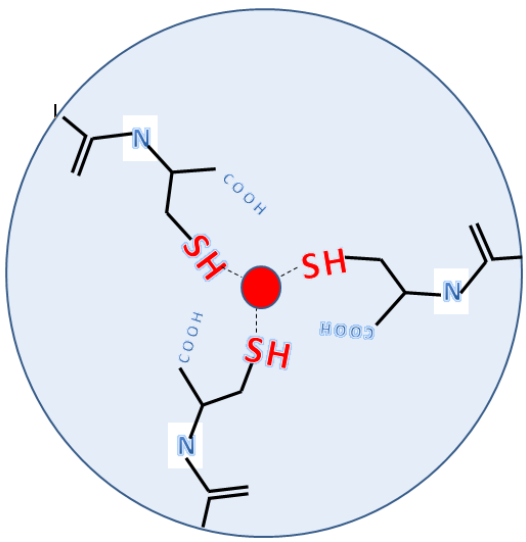

Figure 2. Interaction of arsenic atom and cysteine molecules, predicted As-SH complex.

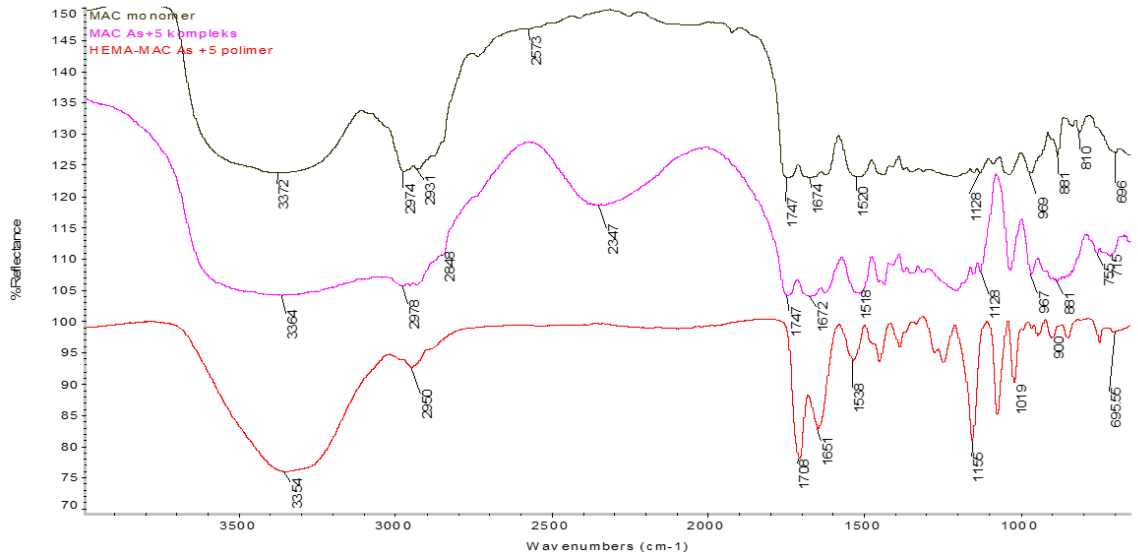

Figure 3. FTIR spectra of MAC monomer, As-MAC complexes and As-IIP cryogel

FTIR spectrum of As-IIP cryogel, there are characteristic hydrogen bond of alcohol, O-H and stretch band around 3354 cm^{-1}, carbonyl band at 1708 cm^{-1}, aliphatic C-H band at 2950 cm^{-1}, and amide I and amide II bands respectively at 1651 cm^{-1} and 1538 cm^{-1}.As can be seen from the FTIR spectra of the synthesized cryogels, the peaks in the polymeric structure are sharper than the peaks in the monomer and complex.The presence of the peaks at 1162 $cm^{-1}$and 967 cm^{-1} belonging to the MAC monomer indicates that the MAC monomer has successfully entered the polymeric structure.

Surface Imaging with SEM

The surface properties of the synthesized As-IIP cryogels were determined by Scanning Electron Microscope (SEM) (Figure 4). These images clearly show that cryogels have a highly porous structure. It is observed that the prepared cryogels have a smooth and uniform surface and interconnected macropores. This macroporosity is in the range of 10-100 µm and ensures that the flow dynamics of the cryogels are quite smooth.

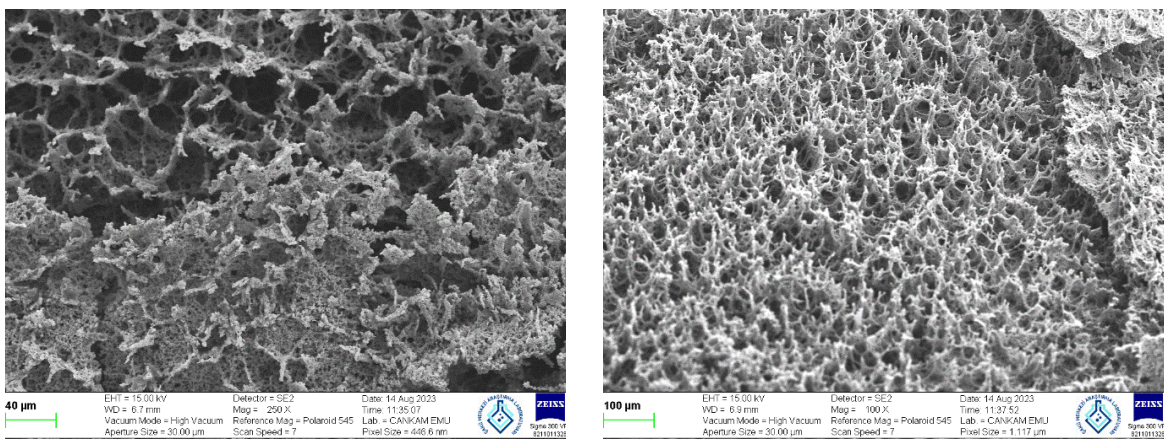

Figure 3. FTIR spectra of MAC monomer, As-MAC complexes and As-IIP cryogel

Table 1. Swelling behavior of synthesized cryogels.

	Equilibrium swelling ratio(%)	Macroporosity(%)
As-IIP	92.5	65.5
NIP	90.5	64.0

Table 2. Elemental analysis results of As-IIP cryogel.

	C %	H %	N %	S %
As-IIP	50.01	7.59	3.21	0.33

Table 3. Surface area results of As-IIP cryogel

	Surface Area (BET)a (m2/g)	Total Pore Volumeb (mL/g)	Average Pore Diameterc (Å)
As-IIP	35.6	0.078	34.7
NIP	24.2	0.038	22.0

Examination of Swelling Properties of Cryogel

The equilibrium swelling properties of As-IIP cryogels prepared in this study are given in Table 1. Both cryogels were synthesized under the same conditions and have similar swelling properties. As-IIP cryogels are spongy structures with interconnected macropores. This situation ensures that the equilibrium swelling ratios are high, as seen in Table 1.

As can be seen from the Table, the swelling behaviors of the imprinted and non-imprinted polymers are very close and similar. In addition to the HEMA monomer, the hydrophilicity is also increased with the addition of the cysteine-containing MAC monomer to the polymer backbone, and the swelling rate is increased accordingly. The swelling rate in cross-linked gels is lower than in other gels. As expected, the swelling ratio of the arsenic-imprinted polymer is higher than that of the non- imprinted polymer, since the surface area of the synthesized polymers is larger than that of the non-imprinted polymer.

Elemental Analysis

Using elemental analysis and sulfur stoichiometry, the % S ratio incorporated into the structure of As-IIP cryogel was measured as 0.33 (Table 2). The amount of MAC was calculated as 192.8 µmol/g dry cryogel. It is known that HEMA and other polymerization components do not contain sulfur and the only source of sulfur in the cryogel is the MAC monomer. The amount of sulfur determined by elemental analysis originates from the MAC groups included in the cryogel structure.

Surface Area Measurements

Surface area and pore size distribution are important parameters in molecularly imprinted polymers. These properties were measured with nitrogen absorption/desorption isotherms at liquid nitrogen temperature and relative pressures (P/P0) between 0.05 and 1.0. Specific surface area, total pore volume and average pore diameter for As-IIP and NIP cryogel are given in Table 3. The specific surface area of As-IIP and NIP cryogels was calculated as 35.6 m^2/g and 24.2 m^2/g, respectively, by the multi-point BET method (Table 3.). The surface area of the As-IIP cryogel increased due to the cavities formed after the removal of the template ion As(V). It can be seen that the average pore diameter of the As-IIP cryogel is 34.7 Å. This shows that the As-IIP cryogel consists of mesopores (20-500 Å). The vast majority of pores are in the range of 25-100 Å, and pores up to 1500 Å are present.

As(V) Adsorption from Aqueous Solutions

Effect of pH

Figure 5 shows the adsorption of As-IIP cryogels at different pH values. In experiments investigating the effect of pH on arsenic adsorption, the pH of the solution was adjusted to the desired value by using 0.1 M HNO_3 and 0.1 M NaOH solutions. In this pH range, the maximum adsorption amount for As-IIP cryogels is 46.3 µg As/g dry cryogel at pH 5.0.

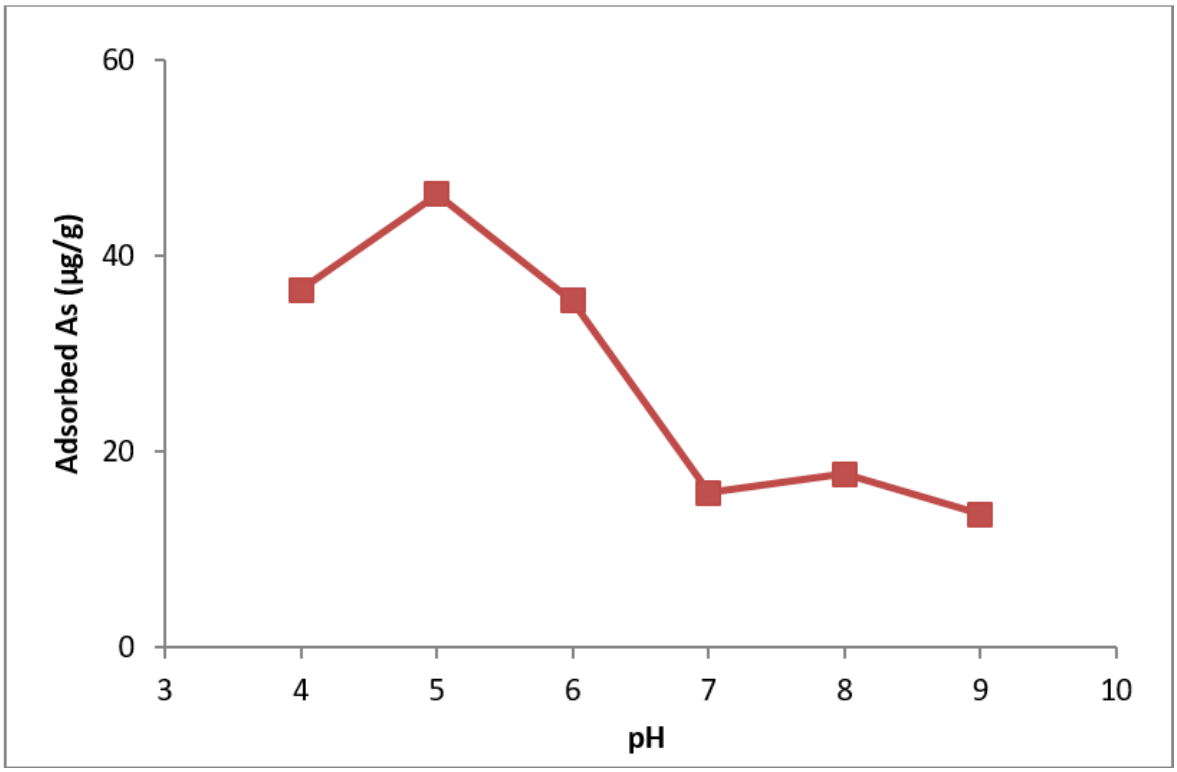

Figure 5. Effect of pH on As(V) adsorption to As-IIP cryogel.

The fact that As-IIP cryogel reaches its maximum value at pH 5.0 can be explained as follows: The isoelectric point of the MAC monomer is 4.9, and the pKa point of the SH group is 8.3. In other words, MAC monomer is in zwitterionic form at approximately pH 5.0, and SH groups switch to anionic form by donating a hydrogen atom to the aqueous medium after pH 8.3. In these two pH ranges, the SH groups of the MAC monomer interact electrostatically with arsenate ions.

In aqueus solution the concentration of arsenate oxyanion ($H_2AsO_4^-$) is at its highest level in the pH range of 4.0-5.0 [1,2]. So arsenate is in anionic form. As shown in Figure 5, a significant decrease ofthe As(V)adsorption is observed after pH 5.0. The decrease in the amount of adsorption continues until pH 7.0. This shows that the electrostatic interactions between MAC monomer and ($H_2AsO_4^-$) oxyanions are intense in the pH range of 4.0-5.0, and as the pH value increases towards 7.0, there is a decrease in adsorption due to the decrease in the concentration of arsenate ions. Because, as stated before, the -SH groups of the MAC monomer interact with arsenate ions. In addition, the slight increase observed in the adsorption graph after pH 7.0 can be explained by the transition of arsenate ions from ($H_2AsO_4^-$) form to ($HAsO_4^{-2}$) form at this pH. This situation can be expressed as follows: as the arsenate ion transitions to the form ($HAsO_4^{-2}$), the interaction of the MAC monomer with SH groups (pKa: 8.3) increases. The decrease observed after this shows that interactions also decrease depending on pH. According to the results obtained from these experiments, the solution pH of As(V) adsorption studies was kept at 5.0 for As-IIP cryogel.

Effect of Flow Rate

Figure 6 shows As(V) adsorption onto As-IIP cryogel at different flow rates. In the flow rate range of 0.5-3.0 mL/min, the maximum As(V) adsorption amount was As-IIP 46.3µg As/g dry cryogel at a flow rate of 0.5 mL/min. It was observed that the amount of As(V) adsorption decreased as the flow rate increased. It was observed that by increasing the flow rate to 3.0 mL/min, the amount of As(V) adsorption decreased to 13.8µg As/g dry cryogel. Increasing the flow rate also reduced the amount of adsorption as it reduced the contact time of the cryogel with the As(V) solution. As a result, a decrease in adsorption capacity is observed as the interaction time and probability of As(V) ions with the As-IIP cryogel will decrease. According to the results obtained from this experiment, other adsorption studies were carried out at a flow rate of 0.5 mL/min.

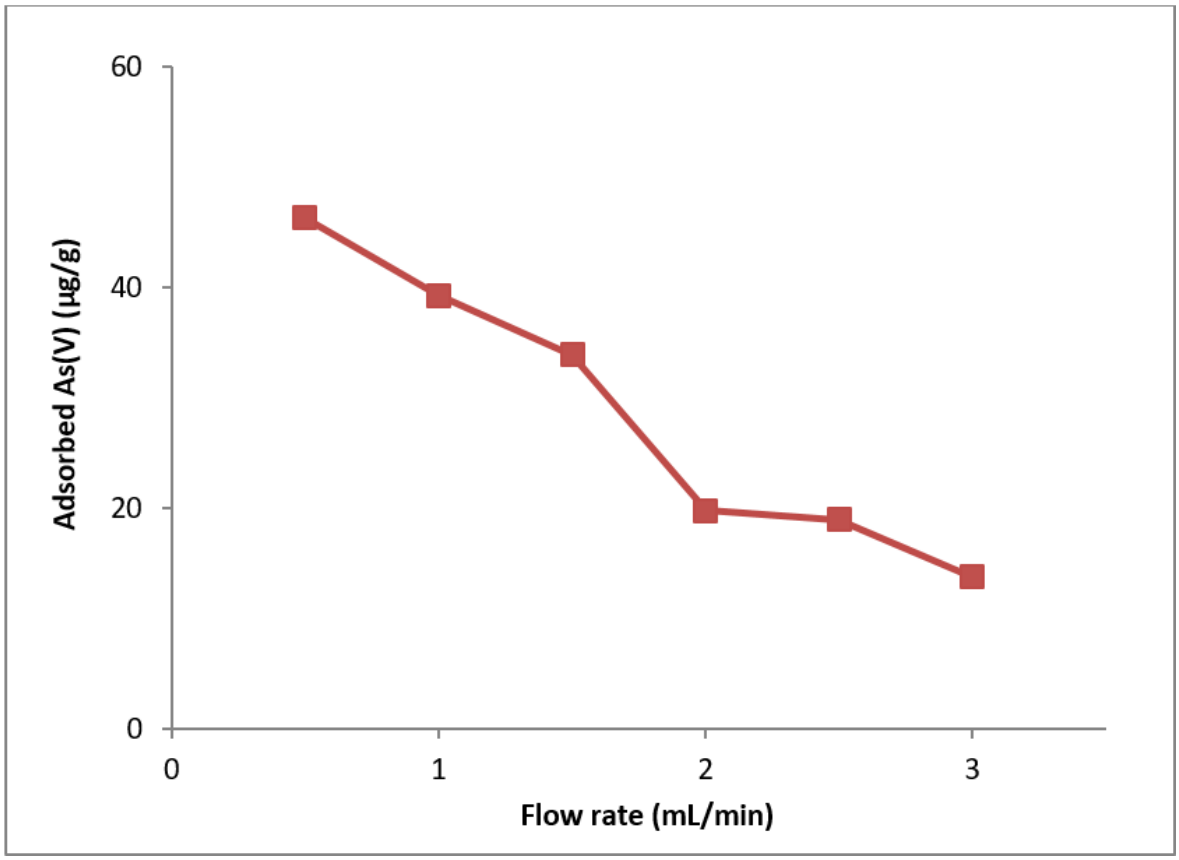

Figure 6. Effect of flow rate on As(V) adsorption.

Effect of Initial Concentration

Figure 7 shows the variation of As(V) adsorption onto As-IIP cryogels with the initial As(V) concentration in the medium. As seen from the Figure 7, with the increase of the initial concentration of As(V) in the solution, the amount of As(V) adsorbed per unit As-IIP cryogel increased rapidly until the initial As(V) value of 5 ppm, and a plateau was reached at the initial concentration of approximately 10ppm As(V) as the specific regions where As ions could bind were filled. As the concentration increases, the concentration difference (ΔC), which is the driving force for adsorption, increases. As the driving force increases, the adsorption capacity also increases. The maximum adsorption capacity of As-IIP cryogels for an initial concentration of 15 ppm As(V) is 189.4µgAs/g dry cryogel. The As(V) removal rate of As-IIP cryogel was recorded as 94% (3µg/L) for 50ppb As solution. This value is below the arsenic limit in drinking water (10µg/L) determined by the EPA [45].

Effect of Adsorption Rate

Figure 8 shows the time-dependent As(V) adsorption. Adsorption occurs quite quickly. As expected, the adsorption capacity reached a plateau in 60 minutes due to the filling of the unique molecular cavities where As(V) ions can bind on the adsorbent surface. During this time, the maximum adsorption amount for As(V) ions was 30.8µg As/g dry IIP cryogel. With the imprinting process, specific cavities for As(V) ions were formed in the As-IIP structure. These As(V) cavities in As-IIP have geometric affinity for As(V) ions in solution and have high complexation abilities.

Effect of Temperature

Figure 9 shows the effect of As(V) adsorption onto As-IIP cryogels at different temperatures. In the study, in the temperature range of 4-40°C, the maximum adsorption was realized at 40°C. For As-IIP cryogel, this value is 48.5µg As/g dry cryogel. With increasing temperature, the interaction between the adsorbent and As(V) increases, thus As(V) adsorption increases.

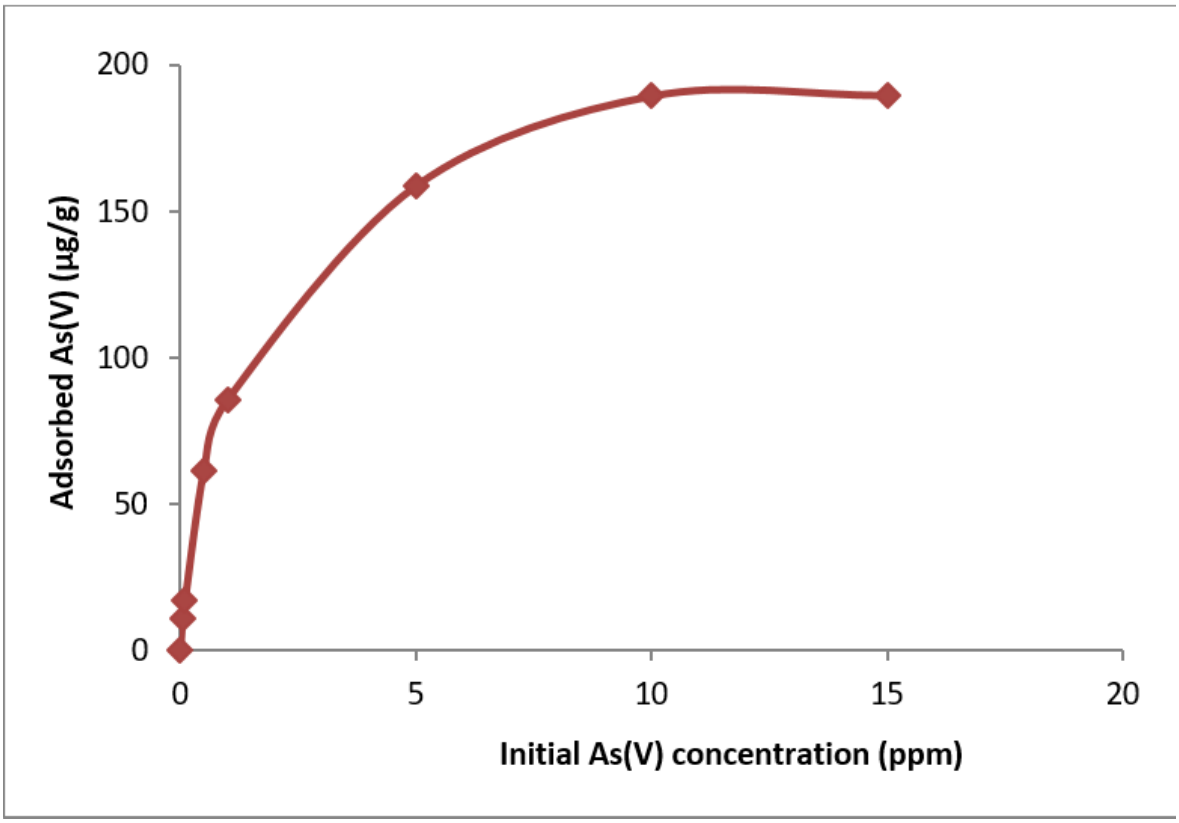

Figure 7. Effect of initial concentration on As adsorption.

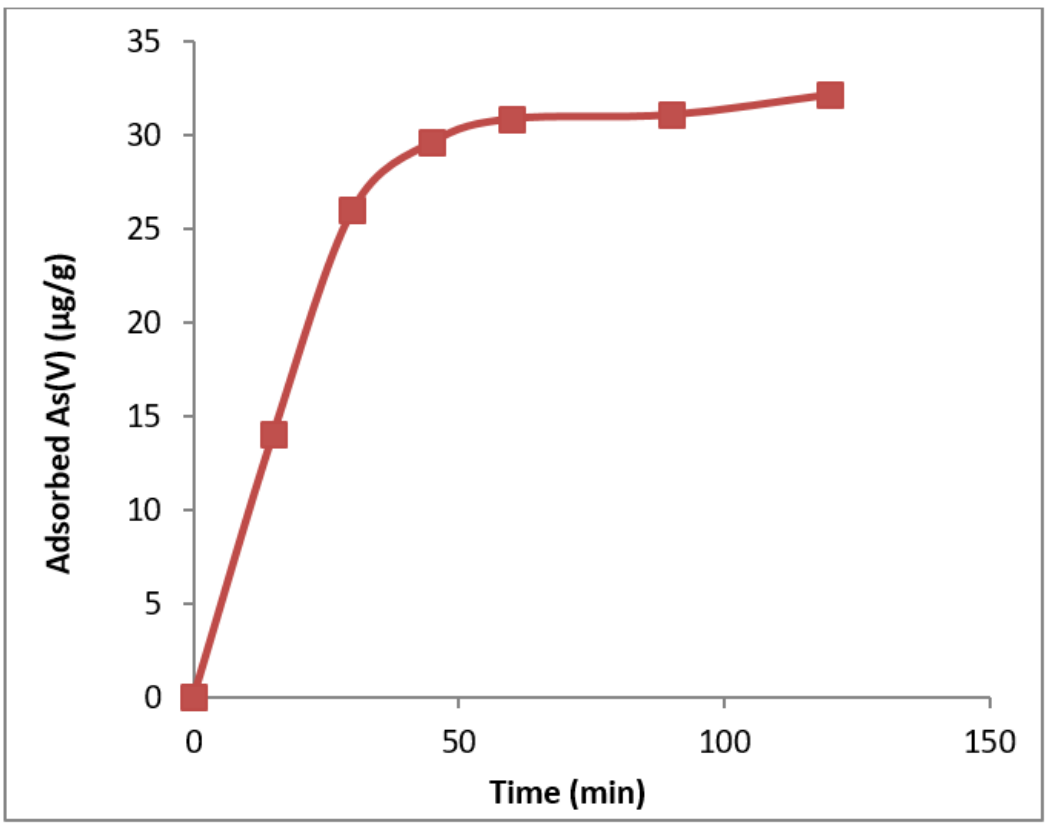

Figure 8. Effect of interaction time on adsorption.

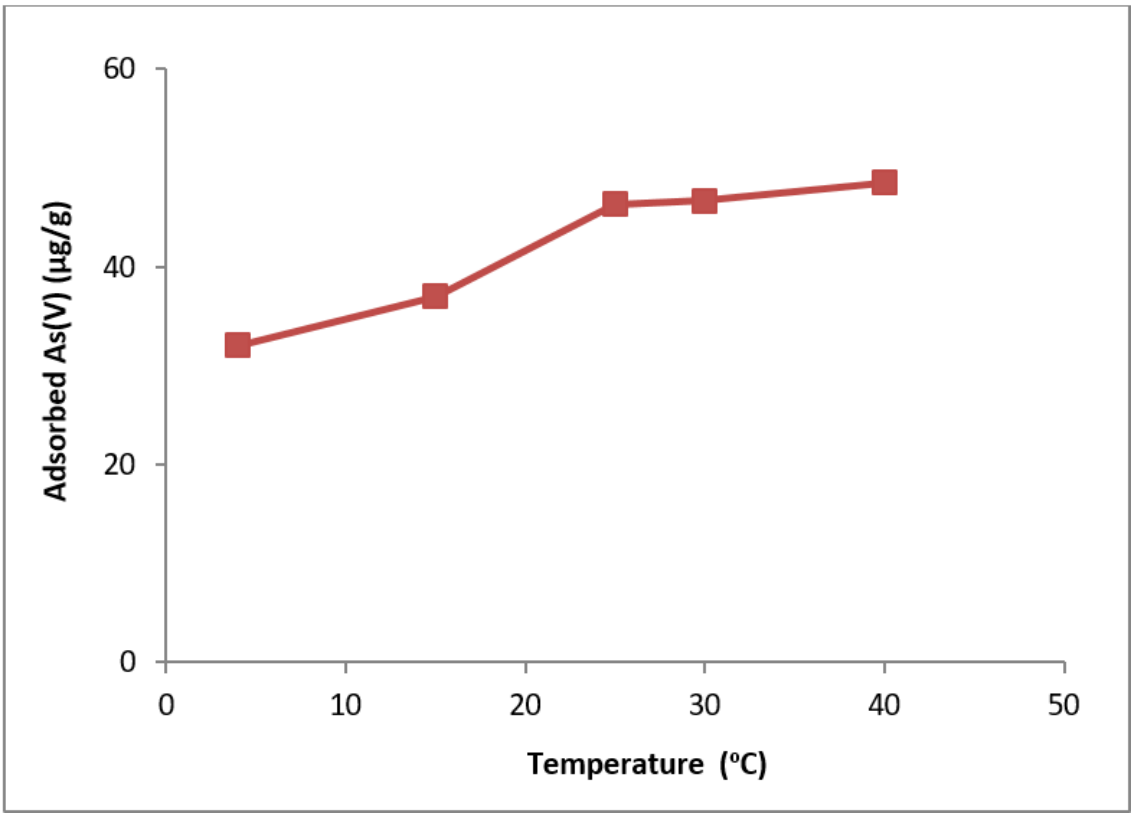

Figure 9. Effect of temperature on As(V) adsorption to As-IIP cryogel.

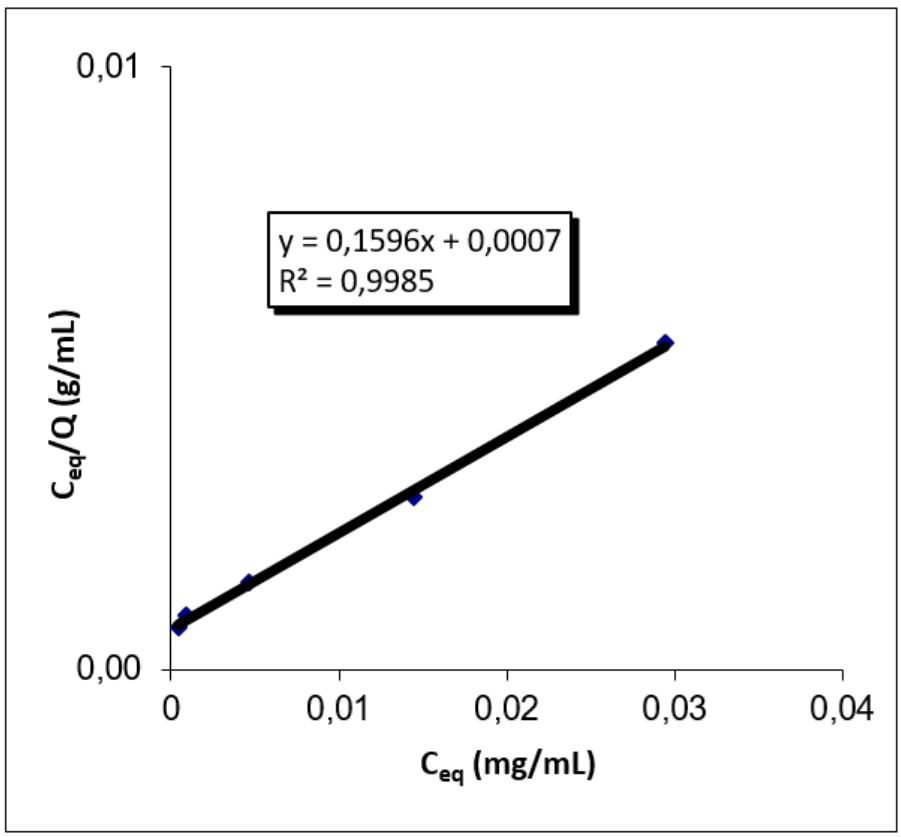

Figure 10. Linear graphs of Langmuir adsorption isotherms for As-IIP cryogels.

Adsorption Isotherms

Adsorption isotherms are mathematical expressions used to describe the relationship between the concentration of ions in solution at equilibrium and the amount of ions adsorbed to the solid phase[46]. Adsorption continues until an equilibrium is established between the the substance accumulated on the adsorbent surface and the concentration of the substance remaining in the solution. Mathematically, this equilibrium is explained by adsorption isotherms. Over time, many researchers have put forward different isotherm equations, based on a general formula created by Jaeger and Erdös. Langmuir and Freundlich equations are the most commonly used isotherms.

The Langmuir adsorption model assumes that molecules bind to a certain number of sites, each of which can bind only a single molecule[47]. It is assumed that these points are equivalent in terms of energy and that there is no interaction between adjacent regions and adsorbed molecules. Langmuir adsorption isotherm is defined by Equation 7. Obtaining a linear graph by applying the equilibrium data to the equation shows that the Langmuir model can be applied to these systems.

$$C_{eq}/Q = 1/(Q_L . b) + C_{eq}/Q_L \quad (7)$$

In this equation, Q indicates the amount of As(V) bound to the As-IIP cryogel (mg/g), C_{eq} indicates the equilibrium As(V) concentration in the solution (mg/mL), b represents the Langmuir constant (mL/mg) and Q_L indicates the adsorption capacity (mg/g). The linear graph of experimental data for As(V) adsorption is given in Figure 10.

The Freundlich equation is another isotherm that describes the most commonly used adsorption behavior in cases where heterogeneous surface energy is involved[48]. It is not limited to monolayer adsorption like the Langmuir adsorption isotherm. The Freundlich equation assumes that the metal adsorption energy to the adsorbent varies depending on whether the neighboring binding sites are occupied or not. Experimentally, Equation 8 is expressed as follows.

$$Q_{eq} = Q_F . C_{eq}^{1/n} \quad (8)$$

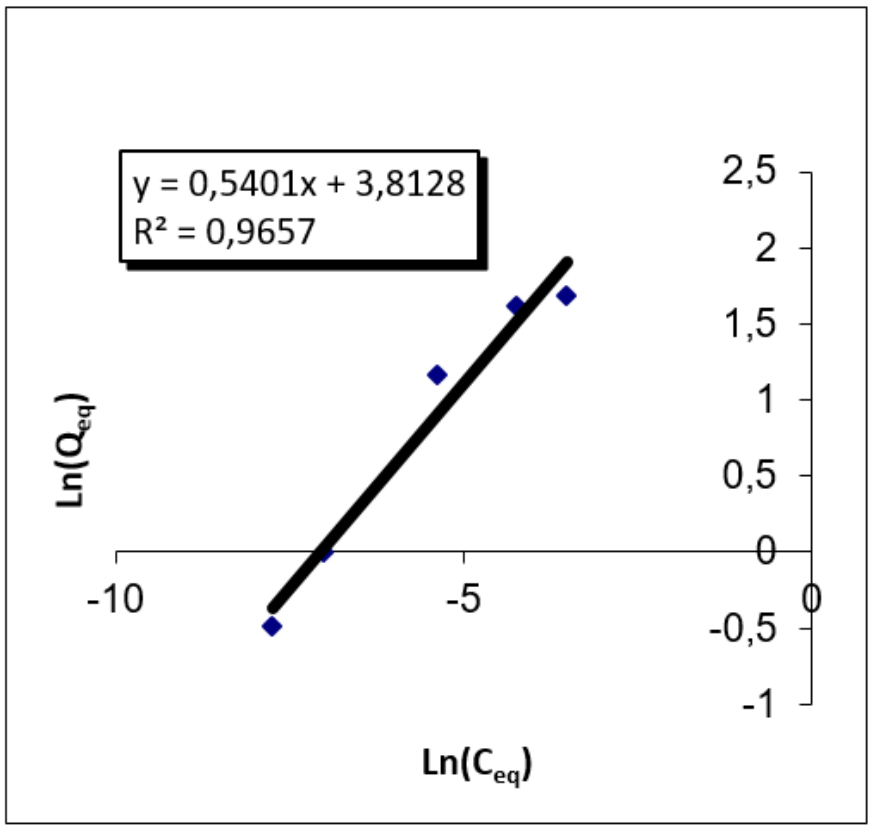

Figure 11. Linear graphs of Freundlich adsorption isotherms for As-IIP cryogels.

In this equation, Q_{eq} refers to the adsorption amount (mg/g), C_{eq} refers to the adsorbent concentration in the solution (mg/L), Q_F refers to the adsorption capacity, and 1/n refers to the Freundlich coefficient showing the heterogeneity of the system. Q_F and 1/n values are calculated by taking the logarithm of the equation (Equation 9) and drawing the linear graph of Ln Q_{eq} against Ln C_{eq} (Figure 11).

$$\ln Q_{eq} = \ln Q_F + 1/n * \ln C_{eq} \quad (9)$$

Table 4 evaluates the results obtained from the linear graphs of Langmuir and Freundlich isotherms. The maximum adsorption capacity calculated from experimental data is 0.189 mg/g dry cryogel. Langmuir theoretical adsorption capacity was calculated as 0.196 mg/g and matches the experimental data. Langmuir correlation coefficients are higher than Freundlich correlation coefficients (R^2 = 0.99). This result shows that the Langmuir adsorption isotherm is more suitable for this system. In addition, the Freundlich isotherm describes reversible adsorption and is not limited to monolayer formation. As the homogeneity of the system increases, the n value approaches 1, and as the heterogeneity increases, the n value approaches zero. Accordingly, the n value calculated in Table 4 indicates that the prepared As-IIP cryogel has homogeneous binding sites, and this result does not agree with the Freundlich adsorption isotherm, which expresses heterogeneous binding sites.

Table 4. Langmuir and Freundlich constants.

	Experimental	Langmuir Constants			Freundlich Constants		
	$Q_{experimental}$	Q_L	B	R_2	Q_F	n	R_2
	(mg/g)	(mg/g)	(mL/mg)		(mg/g)		
As-IIP	0.189	0.196	5.11	0.997	0.41	3.47	0.984

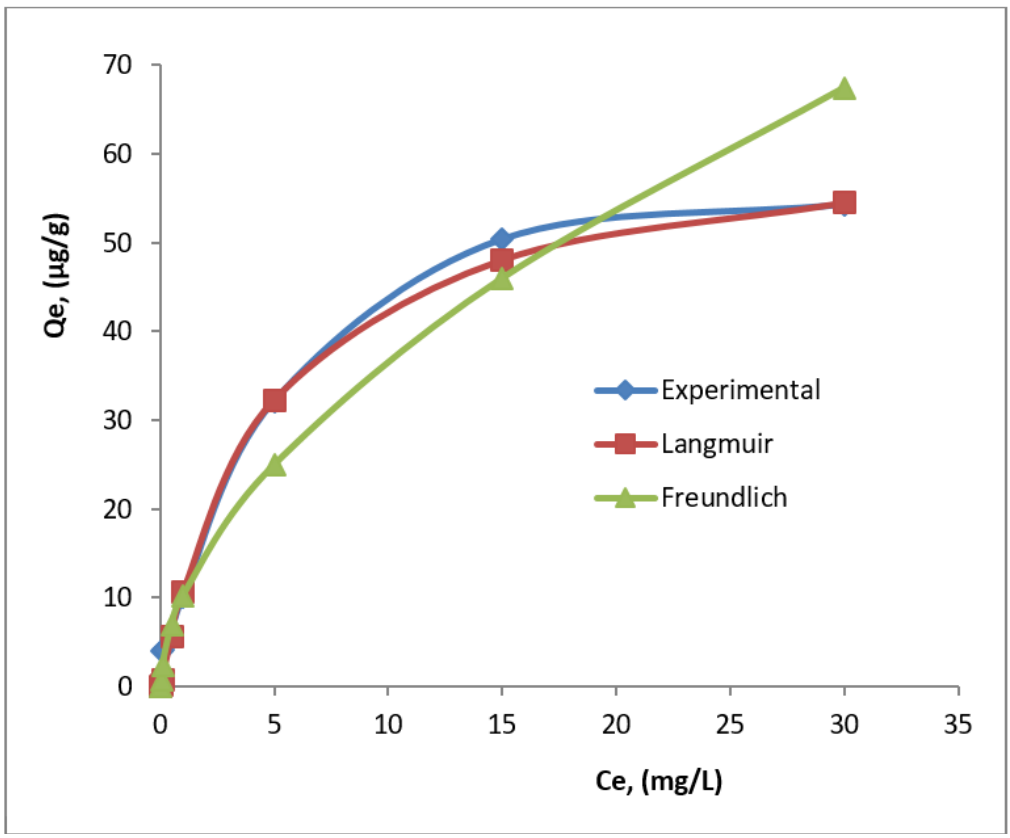

Figure 12. Experimental adsorption capacity (µg/g) of As-IIP cryogels and adsorption capacities modeled by Langmuir and Freundlich.

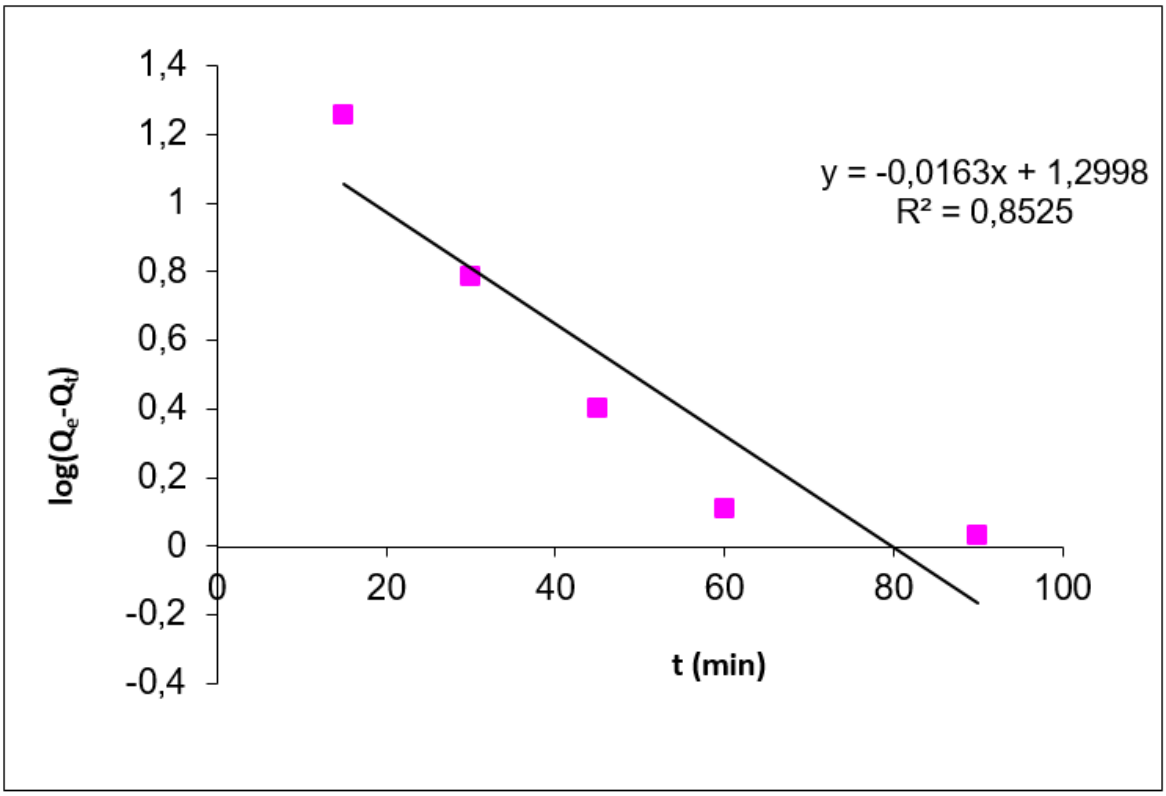

Figure 13. Pseudo-first order graphs of As-IIP cryogels.

Figure 12 compares the experimental adsorption capacity of As-IIP cryogels in µg/g with the adsorption capacities modeled by Langmuir and Freundlich. As seen in the figures, the adsorption behavior of As-IIP cryogels is compatible with the adsorption behavior modeled by Langmuir.

Adsorption Kinetics

Adsorption kinetics determines the effective adsorbent-adsorbed contact time, that is, the retention time. It is an important step to understand the adsorption steps that affect the speed of the adsorption process. First- and second-order kinetic models were applied to the experimental data to determine the mechanisms controlling the adsorption process, such as mass transfer and chemical reaction. It was assumed that the measured concentrations were equal to the surface concentration of the adsorbent. Lagergren's first order rate equation is the most commonly used equation in the adsorption of solute from solution[49]. Equation 10 is expressed as follows.

$$\Delta Qt/dt=k_1(Q_e-Q_t) \quad (10)$$

In the equation, k_1 represents the pseudo-first order adsorption rate constant (min^{-1}), Q_e and Q_t represent the amount of ions (mg/g) adsorbed at equilibrium time and at any time t, respectively. Applying the boundary conditions Q_t = 0 at t = 0 and Q_t = Q_t at time t = t and integrating them gives the equation 11.

$$\log[Q_e/(Q_e-Q_t)]= (k_1t)/2.303 \quad (11)$$

If Equation 11 is rearranged and linearized Equation 12 is obtained.

$$\log(Q_e-Q_t)= \log(Q_e) - (k_1t)/2.303 \quad (12)$$

The linearity of the t plot against $\log(Q_e)$ demonstrates the applicability of the kinetic model. In a true first-order process, $\log(Q_e)$ must equal the intercept of the t plot against $\log(Q_e-Q_t)$. Figure 13 shows the pseudo-first order linear graph of As-IIP cryogels.

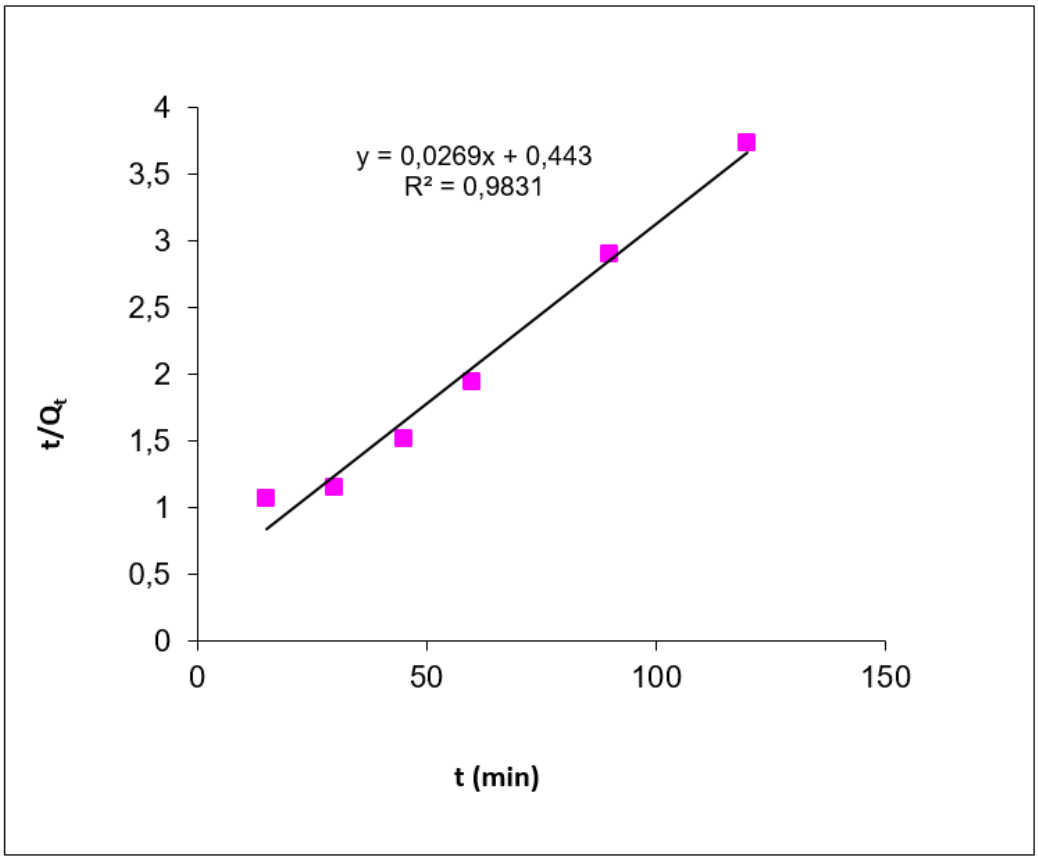

Figure 14. Pseudo-second order graphs of As-IIP cryogels.

In addition, the pseudo-second order equation based on the adsorption equilibrium capacity can be given as follows:

$$\Delta Q_t/dt = k_2 (Q_e-Q_t)^2 \quad (13)$$

In the equation, k_2 is the pseudo-second order rate constant (g.mg^{-1}.min^{-1}). By applying the boundary conditions $Q_t = 0$ at $t = 0$ and $q_t = q_t$ at $t = t$ to Equation 13;

$$1/(Q_e-Q_t)] = (1/Q_e) + k_2 t \quad (14)$$

equation is obtained. The linear form of this equation is expressed as:

$$(t/Q_t)= (1/k_2 Q_e^2) + (1/Q_e)\, t \quad (15)$$

For second-order kinetics to be applicable, the t/q_t versus t plot must be linear. The rate constant (k_2) and equilibrium adsorption (Q_e) can be obtained from the intercept and slope, respectively. Figure 14 shows pseudo-second order linear plots of As-IIP cryogels.

Pseudo-first and second-order kinetic constants of As-IIP cryogels are given in Table 5. As a result of the calculations, it is seen that the second-order kinetic model is more suitable for As(V) in aqueous solutions in As-IIP cryogels. The theoretical Qe values obtained in second-order kinetic calculations are very close to the experimental Qe values. These results show that adsorption of As(V) in aqueous solutions in As-IIP cryogels takes place under chemical control. That is, the adsorption behavior conforming to the pseudo-second-order kinetic model shows that diffusion restrictions are negligible, therefore chemical adsorption, that is, the specific binding reaction between MAC and As(V), controls the kinetic behavior.

Table 5. Pseudo-first and second-order kinetic constants for As-IIP cryogels (Equilibrium concentration: 0.5 mg/L).

	Experimental	1st Order Kinetics			2nd Order Kinetics		
	c (mg/g)	k_1 (1/min)	Q_e (mg/g)	R^2	k_2 (g/mg.min)	Q_e (mg/g)	R^2
As-IIP	62.48	0.050	6.77	0.969	$6.41x10^{-4}$	73.52	0.990

Table 6. K and K' values of As-IIP cryogels in the presence of competitive anions.

	As(V)-IIP	NIP	As-IIP
	K ($K_{D\,As}/K_{D\,Anyon}$)	K (As(V))	K' (K_{IIP}/K_{NIP})
As(V)	-	-	-
PO_4^{3-}	9.12	6.00	1.52
SO_4^{2-}	16.86	6.46	2.61
NO_3^-	12.77	8.36	1.53

Selectivity Experiments

To demonstrate the selectivity of As-IIP cryogel, competitive adsorption experiments were carried out in aqueous solution and continuous system. PO_4^{3-}, SO_4^{2-} and NO_3^- were used as competitive anions. As oxy-anions were added to the competitive anion mixtures.

Table 6 gives the selectivity and relative selectivity coefficients (K and K' values) of As oxyanions for As-IIP and NIP cryogels, respectively. The K value is calculated by the ratio of the distribution coefficient of the imprinted ion ($K_{D\,As}$) to the distribution coefficient of the competing anion ($K_{D\,Anyon}$). As a result of the analyses, it was calculated that the K values of As-IIP cryogels in the presence of competitive anions were higher than the K values of NIP cryogels. The relative selectivity coefficient (K' value) shows the selectivity of the active binding sites of As-IIP cryogels compared to NIP cryogel. Accordingly, when the K' values of As-IIP cryogel are examined, it is seen that it is 1.52, 2.61 and 1.53 times more selective than PO_4^{3-}, SO_4^{2-} and NO_3^- anions, respectively.

In selectivity studies of NIP, As-IIP cryogels, the initial concentrations of competitive anions (PO_4^{3-}, SO_4^{2-} and NO_3^-) and As oxy-anion are 5 mg/L. The amounts of As(V) adsorbed in the presence of these competitive anions are seen in Figure 15. When these results are examined, while As-IIP cryogels show high selectivity for As(V) in the presence of other anions, while As(V) adsorbed to NIP cryogel does not show significant selectivity. However, the amounts of competitive anions adsorbed to As-IIP and NIP cryogels are negligible. These results show that active recognition sites of As-IIP cryogels created for As(V) have successfully synthesized in terms of providing high selectivity over other competitive anions in the solution medium.

Desorption and Reusability

50 mM EDTA (pH: 4.0) solution was used as a desorption agent for the desorption of As(V) ions adsorbed on the As-IIP cryogel. In order to determine the reusability of the As-IIP cryogel, the adsorption-desorption process was repeated at least 10 times using the same cryogel. The adsorption-desorption cycle showing the reusability of As-IIP cryogels is given in Figure 16. In the adsorption study of As-IIP cryogels repeated at least 10 times, the desorption rate was recorded as 95%. The desorption rate is quite high for these cryogels and no significant decrease in As(V) adsorption capacity was observed. The interconnected supermacroporous structure of cryogels is a feature that allows desorption to develop easily. Accordingly, desorption reached equilibrium within 30 minutes.

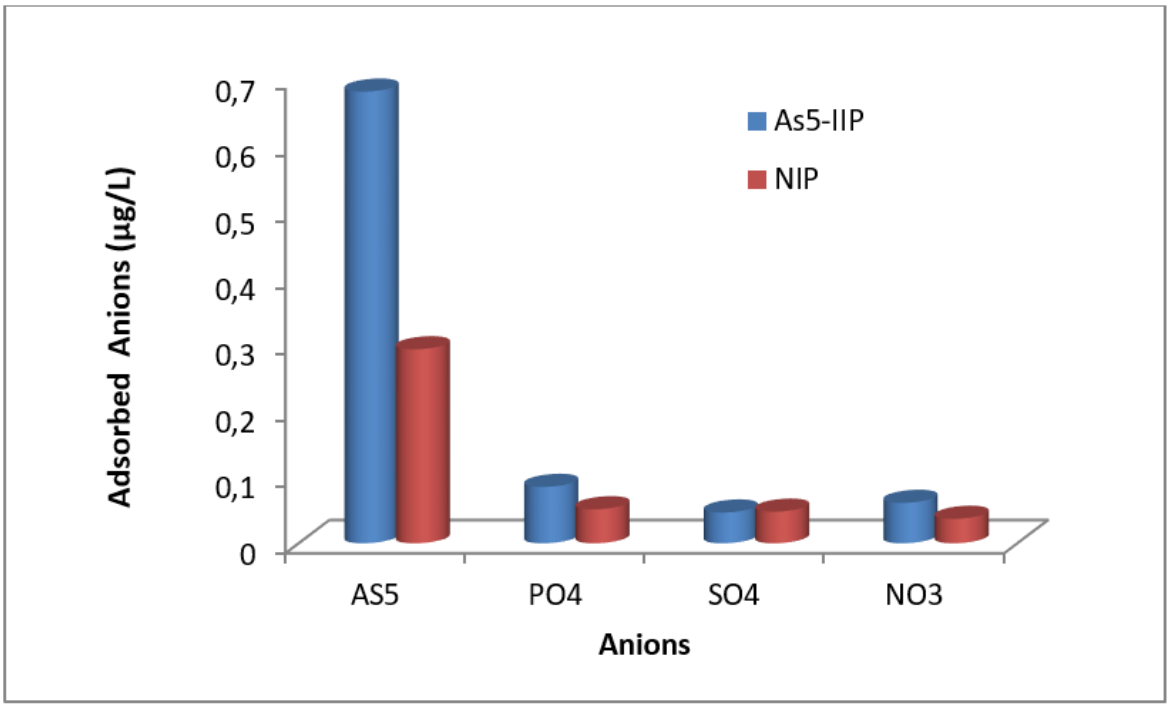

Figure 15. Amounts of As(V) and competitive anions adsorbed to As-IIP and NIP cryogels (mg/L).

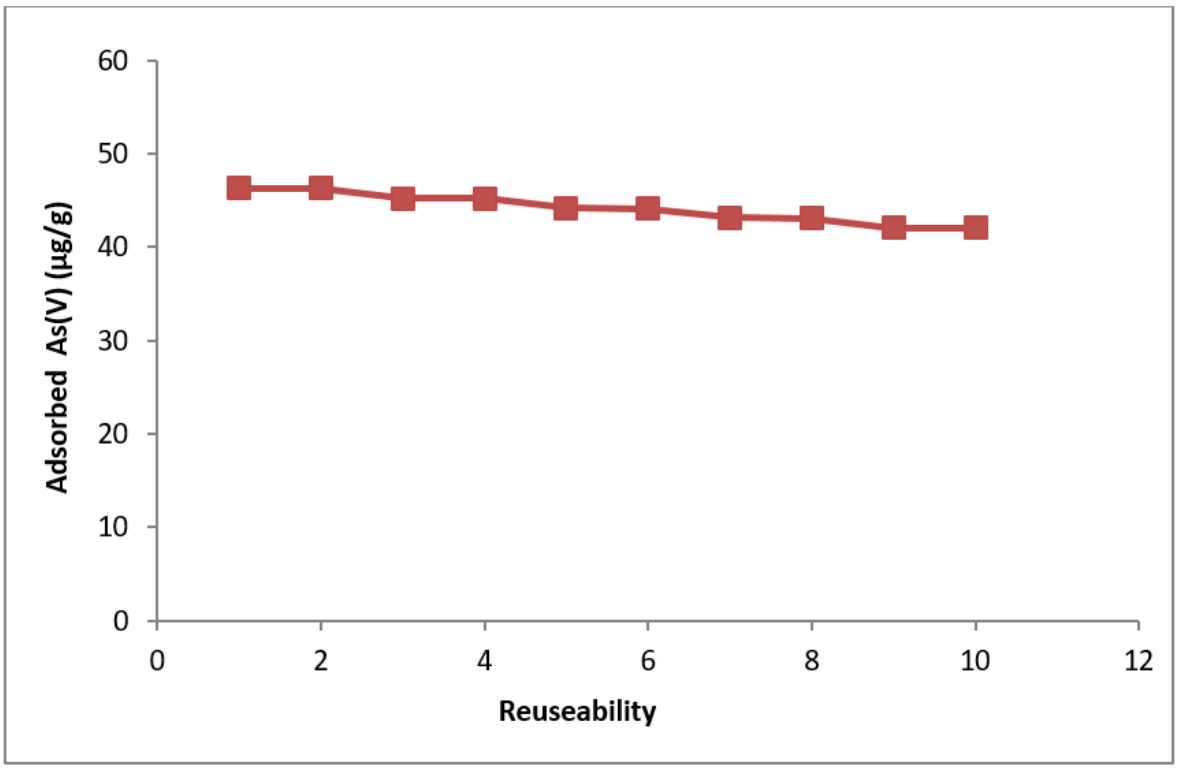

Figure 16. Adsorption-desorption cycle showing the reusability of As-IIP cryogels.

CONCLUSION

As a result of increasing environmental pollution due to increasing human population and industrialization, heavy metal pollution in water is one of the most important problems that concerns all humanity. Heavy metal pollution has reached levels that not only harm the ecosystem but also threaten human health. Arsenic pollution is at the top of the list of heavy metal pollution and is the most harmful. Long-term consumption, especially above the levels determined in drinking water, causes cancer [1-6]. Access to clean water is one of the major unsolved human problems.

In this study, polymeric adsorbents in column form that can be used in tap water were prepared for the removal of arsenic (V), which is a common species in drinking water. Due to its spongy structure, it allows water passage of water without applying pressure and has a high surface area, making the prepared cryogel a potential candidate for water purification.

It was investigated whether poly(HEMA-MAC) cryogel, prepared based on the affinity of arsenic to –SH functional groups, could be used selectively in the removal of arsenic ions from water. The physicochemical properties of the synthesized cryogel were determined through characterization studies. Subsequently, optimum conditions for arsenic removal from water were determined as the maximum adsorption was 189.4µg/g polymer at pH: 5.0, close to neutral pH. In experimental studies, it has been observed that polymeric cryogel selectively removes As(V) ions in the presence of competitive ions such as PO_4^{3-}, SO_4^{2-} ve NO_3^- ions in the medium, which cause problems in arsenic removal by adsorption method. In addition, it is economically important that the synthesized adsorbent can be regenerated and used again and again without losing its adsorption ability. In experimental studies conducted to determine the regeneration and reusability properties of the prepared As-IIP cryogel, it was revealed that the polymeric adsorbent can be used again and again without significant changes in its adsorption capacity.

As a result of all these experimental studies, it can be stated that the synthesized As-IIP polymeric cryogel removes Arsenic ions from drinking water and can easily bring it to the levels required by WHO. As a result, it appears that the synthesized polymeric adsorbent is a candidate with significant potential in removing arsenic from water.

References

1. 1. P.L. Smedley, D.G. Kinniburgh, A Review of the source, behavior and distribution of arsenic in natural waters, Appl. Geochem., 17 (2002) 517-568.
2. 2. D. Mohan, Jr.C.U. Pittman, Review. Arsenic removal from water/wastewater using adsorbents A critical review, J. Hazard. Mater., 142 (2007) 1-53
3. 3. A. Mudhoo, S.K. Sharma, V.K. Garg, C.H. Tseng, Arsenic: An overview of applications, health, and environmental concerns and removal processes, Crit. Rev. Environ. Sci. Technol., 41 (2011) 435-519.
4. 4. T.S. Choong, T.G. Chuah, Y. Robiah, F.G. Koay, I. Azni, Arsenic toxicity, health hazards and removal techniques from water: an overview, Desalination, 217 (2007) 139-166.
5. 5. L. Weerasundara, Y.S. Ok, J. Bundschuh, Selective removal of arsenic in water: A critical review, Environ. Pollut., 268 (2021) 115668.
6. 6. B.S. Rathi, P.S. Kumar, A review on sources, identification and treatment strategies for the removal of toxic Arsenic from water system, J. Hazard. Mater., 418 (2021) 126299.
7. 7. W.A.H. Altowayti, N. Othman, S. Shahir, A.F. Alshalif, A.A. Al-Gheethi, F.A.H. Al-Towayti, S.A. Haris, Removal of arsenic from wastewater by using different technologies and adsorbents: A review, Int. J. Environ. Sci. Technol., (2021) 1-24.
8. 8. R. Singh, S. Singh, P. Parihar, V.P. Singh, S.M Prasad, Arsenic contamination, consequences and remediation techniques: a review, Ecotoxicol. Environ. Saf., 112 (2015) 247-270.
9. 9. F. Dilpazeer, M. Munir, M.Y.J. Baloch, I. Shafiq, J. Iqbal, M. Saeed, I. Mahboob, A comprehensive review of the latest advancements in controlling arsenic contaminants in groundwater, Water, 15 (2023) 478.
10. 10. S. Alka, S. Shahir, N. Ibrahim, M.J. Ndejiko, D.V.N. Vo, F. Abd Manan, Arsenic removal technologies and future trends: A mini review, J. Clean. Prod., 278 (2021) 123805.
11. 11. H. Rahidul Hassan, A review on different arsenic removal techniques used for decontamination of drinking water, Environ. Pollut. Bioavailab., 35 (2023) 2165964.
12. 12. M. F. Ahmed, An overview of arsenic removal technologies in Bangladesh and India, Proceedings of BUET-UNU international workshop on technologies for arsenic removal from drinking water, Dhaka, (2001) 5-7.
13. 13. P.M. Kirisenage, S.M. Zulqarnain, J.L. Myers, B.D. Fahlman, A. Mueller, I. Marquez, Development of adsorptive membranes for selective removal of contaminants in water, Polymers, 14 (2022) 3146.
14. 14. M. Chen, K. Shafer-Peltier, S.J. Randtke, E. Peltier, Modeling arsenic (V) removal from water by micellar enhanced ultrafiltration in the presence of competing anions, Chemosphere, 213 (2018) 285-294.
15. 15. R.J.J. Chia, W.J. Lau, N. Yusof, H. Shokravi, A.F. Ismail, Adsorptive membranes for arsenic removal–principles, progress and challenges, Sep. Purif. Rev., 52(2023) 379-399.
16. 16. M.R. Awual, M.A. Hossain, M.A. Shenashen, T. Yaita, S. Suzuki, A. Jyo, Evaluating of arsenic(V) removal from water by weak-base anion exchange adsorbents, Environ. Sci. Pollut. Res. Int., 20 (2013) 421-430.
17. 17. Y. Wang, D.C. Tsang, Effects of solution chemistry on arsenic (V) removal by low-cost adsorbents, J. Environ. Sci., 25(2013) 2291-2298.

18. 18. I. Ali, New generation adsorbents for water treatment, Chem. Rev., 112 (2012) 5073-5091.
19. 19. Y. Wang, D.C. Tsang, Effects of solution chemistry on arsenic (V) removal by low-cost adsorbents, J. Environ. Sci., 25(2013) 2291-2298.
20. 20. G. Crini, E. Lichtfouse, L.D. Wilson, N. Morin-Crini, Conventional and non-conventional adsorbents for wastewater treatment, Environ. Chem. Lett., 17 (2019) 195-213.
21. 21. G. Ertürk, B. Mattiasson, Cryogels-versatile tools in bioseparation, J. Chromatogr. A, 1357(2014) 24-35.
22. 22. D. Türkmen, M. Bakhshpour, S. Akgönüllü, S. Aşır, A. Denizli, Heavy metal ions removal from wastewater using cryogels: A review, Front. Sustain., 3 (2022) 765592.
23. 23. A. Baimenov, D.A. Berillo, S.G. Poulopoulos, V.J. Inglezakis, A review of cryogels synthesis, characterization and applications on the removal of heavy metals from aqueous solutions, Adv. Colloid Interface Sci., 276 (2020) 102088
24. 24. M. Bakhshpour, N. Idil, I. Perçin, A. Denizli, Biomedical applications of polymeric cryogels, Appl. Sci., 9 (2019) 553.
25. 25. L.O. Jones, L. Williams, T. Boam, M. Kalmet, C. Oguike, F.L. Hatton, Cryogels: recent applications in 3D-bioprinting, injectable cryogels, drug delivery, and wound healing, Beilstein J. Org. Chem., 17(2021) 2553-2569.
26. 26. M.E. Han, S.H. Kim, H.D. Kim, H.G. Yim, S.A. Bencherif, T.I. Kim, N.S. Hwang, Extracellular matrix-based cryogels for cartilage tissue engineering, Int. J. Biol. Macromol., 93 (2016) 1410-1419.
27. 27. J. Li, Y. Wang, L. Zhang, Z. Xu, H. Dai, W. Wu, Nanocellulose/gelatin composite cryogels for controlled drug release, ACS Sustain. Chem. Eng., 7 (2019) 6381-6389.
28. 28. M. Andaç, I.Y. Galaev, A. Denizli, Affinity based and molecularly imprinted cryogels: Applications in biomacromolecule purification, J. Chromatogr. B, 1021 (2016) 69-80.
29. 29. L. Önnby, V. Pakade, B, Mattiasson, H. Kirsebom, Polymer composite adsorbents using particles of molecularly ımprinted polymers or aluminium oxide nanoparticles for treatment of arsenic contaminated waters, Water Res., 46 (2012) 4111-4120.
30. 30. I.N. Savina, C.J. English, R.L. Whitby, Y. Zheng, A. Leistner, S.V. Mikhalovsky, A.B. Cundy, High efficiency removal of dissolved As (III) using iron nanoparticle-embedded macroporous polymer composites, J. Hazard. Mater., 192 (2011) 1002-1008.
31. 31. L. Önnby, C. Svensson, L. Mbundi, R. Busquets, A. Cundy, H. Kirsebom, γ-Al2O3-based nanocomposite adsorbents for arsenic (V) removal: Assessing performance, toxicity and particle leakage, Sci. Total Environ., 473 (2014) 207-214.
32. 32. L. Chen, X. Wang, W. Lu, X. Wu, J. Li, Molecular imprinting: perspectives and applications, Chem. Soc. Rev., 45 (2016) 2137-2211.
33. 33. S. Jakavula, N. R. Biata, K. M. Dimpe, V. E. Pakade, P. N. Nomngongo, A critical review on the synthesis and application of ion-imprinted polymers for selective preconcentration, speciation, removal and determination of trace and essential metals from different matrices, Crit Rev. Anal. Chem., 52 (2022) 314-326.
34. 34. Y. El Ouardi, A. Giove, M. Laatikainen, C. Branger, K. Laatikainen, Benefit of ion imprinting technique in solid-phase extraction of heavy metals, special focus on the last decade, J. Environ. Chem. Eng., 9 (2021) 106548.
35. 35. Ö. Erdem, Y. Saylan, M. Andaç, A. Denizli, Molecularly imprinted polymers for removal of metal ions: An alternative treatment method, Biomimetics, 3 (2018) 38
36. 36. L. Wang, M. Pagett, W. Zhang, Molecularly imprinted polymer (MIP) based electrochemical sensors and their recent advances in health applications, Sens. Actuators Rep., 5 (2023) 100153.
37. 37. D. Cunliffe, A. Kirby, C. Alexander, Molecularly imprinted drug delivery systems, Adv. Drug Deliv. Rev., 57 (2005) 1836-1853.
38. 38. D. Türkmen, M. Özkaya Türkmen, S Akgönüllü, A. Denizli Development of ion imprinted based magnetic nanoparticles for selective removal of arsenic (III) and arsenic (V) from wastewater, Sep. Sci. Technol., 57 (2022) 990-999.
39. 39. M.C. Teixeira, V.S.T. Ciminelli, M.S.S. Dantas, S.F. Diniz, H.A. Duarte, Raman spectroscopy and dft calculations of as(ıı) complexation with a cysteine-rich biomaterial, J. Colloid Interface Sci., 315 (2007) 128-134.
40. 40. S. Shen, X.F. Li, W.R. Cullen, M. Weinfeld, X.C. Le, Arsenic binding to proteins, Chem. Rev., 113 (2013) 7769-7792.
41. 41. D. Picón, N. Torasso, J.R.V. Baudrit, S. Cerveny, S. Goyanes, Bio-inspired membranes for adsorption of arsenic via immobilized L-Cysteine in highly hydrophilic electrospun nanofibers, Chem. Eng. Res. Des., 185 (2022) 108-118.
42. 42. M. Tripathy, S. Padhiari, G. Hota, L-Cysteine-functionalized mesoporous magnetite nanospheres: synthesis and adsorptive application toward arsenic remediation, J. Chem. Eng. Data., 65 (2020) 3906-3919.
43. 43. S. Özkara, M. Andaç, V. Karakoç, R. Say, A. Denizli, Ion-imprinted PHEMA based monolith for the removal of Fe3+ ions from aqueous solutions, J. Appl. Polym. Sci., 120 (2011) 1829-1836.
44. 44. V. Karakoç, D. Türkmen, H. Shaikh, N. Bereli, C.A. Andac, A. Denizli, Synthesis and Characterization of Poly N-isopropylacrylamide Thermosensitive Based Cryogel, Hacettepe J. Biol. Chem., 41 (2013) 159-166.
45. 45. L. Uzun, D. Türkmen, V. Karakoç, H. Yavuz, A. Denizli, Performance of protein-A-based affinity membranes for antibody purification. J. Biomater. Sci. Polym. Ed., 22 (2011) 2325-2341.
46. 46. EPA, 2001, Arsenic and Clarifications to Compliance and New Source Contaminants Monitoring; Final Rule (66 FR 6976), U.S. Environmental Protection Agency, USA, 174p,.
47. 47. N.E. Labrou, Y.D. Clonis, The interaction of Candida boidinii formate dehydrogenase with a new family of chimeric biomimetic dye-ligands, Arch. Biochem. Biophys., 316 (1995) 169-178.
48. 48. G.M. Finette, Q.M. Mao, M.T. Hearn, Comparative studies on the isothermal characteristics of proteins adsorbed under batch equilibrium conditions to ion-exchange, immobilised metal ion affinity and dye affinity matrices with different ionic strength and temperature conditions, J. Chromatogr. A, 763 (1997) 71-90.
49. 49. R.J. Umpleby, S.C. Baxter, Y. Chen, R.N. Shah, K.D. Shimizu, Characterization of molecularly imprinted polymers with the Langmuir– Freundlich isotherm, Anal. chem., 73 (2001) 4584-4591.
50. 50. C.W. Cheung, J.F. Porter, G. Mckay, Sorption kinetic analysis for the removal of cadmium ions from effluents using bone char, Water Res., 35 (2001) 605-612.
51. 51. V. Karakoç, E. Erçağ. New generation nanoadsorbents and conventional techniques for arsenic removal from waters, JOTCSA, 11 (2024) 845-68.